# Effects of collisions and finite ion temperature on the sheath structure of cylindrical probes in low-pressure electronegative discharges

T. H. Chung[a)]
*Department of Physics, Dong-A University, Busan 604-714, Republic of Korea*

(Received 24 July 2007; accepted 11 April 2008; published online 17 June 2008)

The spatial distributions of electric potential and velocity and density of positive ions are calculated in the surroundings of a negatively biased cylindrical probe immersed in electronegative plasmas. The model equations are solved on the scale of the electron Debye length. The solutions provide the variation of plasma variables along the distance from the plasma bulk region to the probe surface. The control parameters are the ratio of the negative ion density to the electron density, the ratios of the electron temperature to the positive and negative ion temperatures, and the ratio of the rate coefficient for the momentum transfer collision to that for the ionization. Especially, the effects of collision and finite temperature of positive ions are investigated. As the positive ion temperature increases, the sheath width decreases and the positive ion current collected by the probe increases. As the ratio of the rate coefficient for the momentum transfer collision to that for the ionization increases, the sheath edge approaches the plasma region, and the positive ion current to the probe decreases. © *2008 American Institute of Physics*. [DOI: 10.1063/1.2939578]

## I. INTRODUCTION

Electronegative gases such as oxygen, chlorine, $SF_6$, and fluorocarbons are used extensively in electric discharges for various applications of plasma processing. The presence of negative ions complicates the discharge phenomena. There has been an increased demand to determine the plasma parameters such as charged particle densities, sheath width, electron temperature, and plasma potential for electronegative plasmas.[1–3]

Most of the important plasma parameters such as densities of charged species, electron temperature, plasma potential, and electron energy distribution function are obtained from Langmuir probe measurement. The ion saturation zone of the $I-V$ characteristics of the probe is increasingly used in plasma diagnosis. The current drained by the probe in this zone is very small and reduces the perturbation that the measurement causes in the plasma. The interpretation of $I-V$ probe data depends on modeling of the motion of charged species and sheath characteristics. In order to interpret the probe measurements appropriately, it is important to have a realistic theoretical model.[4]

The main issue lies in the modeling of the positive ion flux to the probe for electronegative plasmas. Until now, the positive ions are modeled as a cold, collisionless, or weakly collisional fluid, while both the electron and negative ion densities obey Boltzmann relations. To implement a proper probe theory, one has to solve Poisson's equation for the electric potential and the equations for continuity and momentum balance of positive ions everywhere from the probe surface to $r=\infty$.

The theoretical model of the sheath structure for cylindrical and spherical probes immersed in low-pressure electronegative plasmas has been developed by several authors.[5–12] In a previous paper,[13] a fluid model for collisionless plasmas with cold positive ions was developed for studying the structure of plasma-wall boundaries in low-pressure electronegative plasmas.

In this study, the spatial distributions of electric potential, velocity, and density of positive ions are calculated in the surroundings of a negatively biased cylindrical probe immersed in electronegative plasmas. The model equations are solved on the scale of the electron Debye length. The solutions provide the variation of plasma variables along the distance from the plasma bulk region to the probe surface. The control parameters are the ratio of the negative ion density to the electron density, the ratio of the electron temperature to the positive ion temperatures, and the ratio of the rate coefficient for the momentum transfer collision to that for the ionization. The positive ion current to the probe surface is also calculated. The effects of collision and finite thermal motion of the positive ions are also investigated. The effect of the non-neutrality parameter, defined as the ratio between the Debye length and the ionization length, is also discussed. These issues have also been analyzed by several authors in different approaches.[12,14–18]

It has been shown that collisions of positive ions with neutrals produce an increase of the ion current collected by the probe at lower pressures due to the destruction of the orbital motion and a decrease at higher pressures due to the scattering effect.[4] However, in this study, the ratio of the rate coefficient for the momentum transfer collision to that for the ionization is introduced as a control parameter for the simulation. Therefore, the effect of gas pressure is not considered.

## II. FORMULATION

The plasma variables are calculated along the distance from the plasma region to any arbitrary small distance near the probe edge. A set of coupled equations is formulated, including the steady-state fluid equations of continuity and

[a)]Electronic address: thchung@dau.ac.kr.

 

motion for the positive ion, a Poisson equation with Boltzmann electron, and a Boltzmann negative ion.[7,8] The positive ions are assumed to be all drawn radially into the probe.

A fluid model is developed without the quasi-neutral approximation to solve the spatial distributions of the electric potential and the density and velocity of positive ions in the surroundings of a cylindrical probe immersed in electronegative plasmas. For simplicity, it is assumed that electronegative plasma consists of three charged species, which are positive ion, negative ion, and electron. The basic equations for the positive ions are continuity

$$\nabla \cdot [n_+ \mathbf{v}_+] = \nu_{iz} n_e \tag{1}$$

and the equation of momentum transfer

$$m_+ n_+ \mathbf{v}_+ \cdot \nabla \mathbf{v}_+ = e n_+ \mathbf{E} - \nabla p_+ - m_+ n_+ \nu_c \mathbf{v}_+, \tag{2}$$

where $n_+$, $m_+$, $p_+$, and $\mathbf{v}_+$ are the density, the mass, the pressure, and the velocity of the positive ion, $n_e$ is the electron density, $\nu_{iz}$ and $\nu_c$ are the ionization frequency and the momentum-transfer collision frequency, respectively, and $\mathbf{E}$ is the electric field.

The Poisson's equation is written as

$$\varepsilon_0 \nabla \cdot \mathbf{E} = e(n_+ - n_e - n_-), \quad \mathbf{E} = -\nabla V, \tag{3}$$

where $\varepsilon_0$ is the permittivity of the vacuum, $n_-$ is the negative ion density, $e$ is the electron charge, and $V$ is the electric potential.

Electrons and negative ions are assumed to follow the Boltzmann energy distribution,

$$n_e = n_{e0} \exp\left(\frac{eV}{kT_e}\right), \tag{4}$$

$$n_- = n_{-0} \exp\left(\frac{eV}{kT_-}\right), \tag{5}$$

where $T_e$ and $T_-$ are the temperature of the electrons and the negative ions, respectively, and $k$ is the Boltzmann constant. The subscript 0 indicates the value at the plasma region.

The model equations are developed for a cylindrical electrode (probe) with the assumption that positive ions move radially toward the probe. The isothermal positive ion flow is assumed. The neutral gas density and the temperatures of the electrons and negative ions are taken as constant.

The variation of plasma variables in the plasma-wall transition region can be characterized with several scale lengths.[19] The ionization length or the ion mean-free path can be used for observing the variation of plasma variables in the presheath region. The electron Debye length can be used as a scale length for the sheath region since the sheath width extends only a few electron Debye lengths. On the sheath scale (or electron Debye length scale), the presheath is infinitely remote and sheath edge is characterized by a vanishing field.

The solution of the model equations describes the structure of the sheath region around a cylindrical electrode. We have the dimensionless variables and parameters,

$$\xi = \frac{r}{\lambda_D}, \quad \tilde{n} = \frac{n_+}{n_{e0}}, \quad u = -\frac{v_+}{c_s}, \quad \eta = -\frac{eV}{kT_e},$$
$$\alpha_0 = \frac{n_{-0}}{n_{e0}}, \quad \gamma_- = \frac{T_e}{T_-}, \quad \gamma_+ = \frac{T_e}{T_+}, \quad q = \frac{\lambda_D}{\Lambda}, \quad \delta = \frac{\nu_c}{\nu_{iz}}. \tag{6}$$

where $r$ denotes the radial position in the cylindrical coordinates with the origin at the center of the probe, $c_s$ is the Bohm velocity $(=\sqrt{kT_e/m_+})$, $\lambda_D$ is the electron Debye length, $\Lambda = c_s/\nu_{iz}$ is the ionization length, and $T_+$ is the temperature of positive ions. The $q$ is sometimes called the non-neutrality parameter.

The dimensionless equations of continuity and momentum balance for positive ion and Poisson's equation in cylindrical coordinate are written

$$\frac{d}{d\xi}(\tilde{n}u) + \frac{\tilde{n}u}{\xi} = -qe^{-\eta}, \tag{7}$$

$$\left(u - \frac{1}{\gamma_+ u}\right)\frac{du}{d\xi} = \varepsilon + \frac{1}{\gamma_+ \xi} + \frac{qe^{-\eta}}{\gamma_+ \tilde{n}u} + qu\delta, \tag{8}$$

$$\frac{d\varepsilon}{d\xi} + \frac{\varepsilon}{\xi} = [\tilde{n} - e^{-\eta} - \alpha_0 e^{-\gamma_- \eta}], \tag{9}$$

$$\frac{d\eta}{d\xi} = \varepsilon. \tag{10}$$

If the ionization source term in the continuity equation is neglected, Eq. (7) is reduced to

$$\frac{d}{d\xi}(\xi \tilde{n} u) = 0. \tag{11}$$

Then we have a conserved quantity

$$\xi \tilde{n} u = a(1 + \alpha_0), \tag{12}$$

where

$$a = \frac{j_D}{e n_{+0} c_s},$$
$$j_D = \frac{I_+}{2\pi \lambda_D}. \tag{13}$$

Here, $I_+ = 2\pi e r n_+ v_+$ is the positive ion current to the cylindrical probe per unit length. Then the Poisson equation can be replaced with

$$\frac{d\varepsilon}{d\xi} + \frac{\varepsilon}{\xi} = \frac{a(1+\alpha_0)}{u\xi} - e^{-\eta} - \alpha_0 e^{-\gamma_- \eta}. \tag{14}$$

This equation, combining with the equation of motion, Eq. (8), with $\gamma_+ \to \infty$, $\delta = 0$, has been used to obtain the theoretical $I-V$ characteristic curve of the probe.[5,9] This is an extension of the cold-ion theory of Allen–Boyd–Reynolds (ABR).[20–22]

In the quasi-neutral region, the differential term of the Poisson Eq. (9) may be neglected. Then, we have

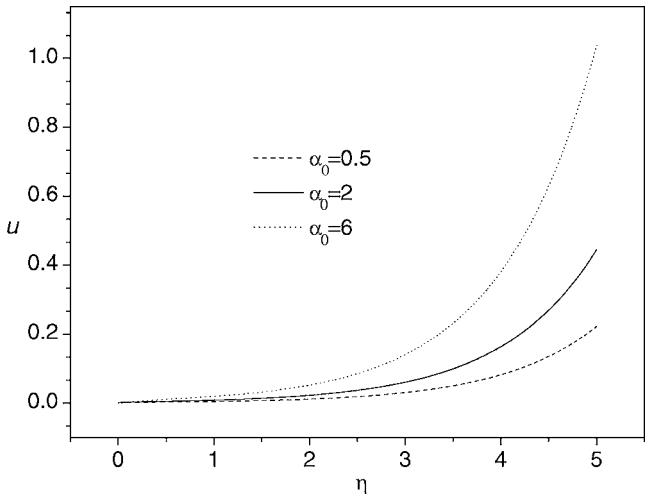


FIG. 1. The evolution of $u$ with $\eta$ near the plasma sheath transition region for various $\alpha_0$ values ($\alpha_0$=0.5, 2, and 6). Here, $a$=90, $\gamma_+$=30, $\gamma_-$=10, $\delta$=0.5.

$$\frac{a(1+\alpha_0)}{u\xi} - e^{-\eta} - \alpha_0 e^{-\gamma_- \eta} = 0. \tag{15}$$

Using Eq. (15) and its differentiation with respect to $\xi$, we can eliminate $\xi$ and $d\eta/d\xi$ from Eq. (8) to obtain

$$\left(u + \frac{a(1+\alpha_0)\delta}{u(e^{-\eta}+\alpha_0 e^{-\gamma_-\eta})}\right)\frac{du}{d\eta} = 1 + \frac{1}{\gamma_+}\frac{e^{-\eta}+\alpha_0\gamma_- e^{-\gamma_-\eta}}{e^{-\eta}+\alpha_0 e^{-\gamma_-\eta}} + \frac{a(1+\alpha_0)\delta(e^{-\eta}+\alpha_0\gamma_- e^{-\gamma_-\eta})}{(e^{-\eta}+\alpha_0 e^{-\gamma_-\eta})^2}. \tag{16}$$

It should be noted that the velocity of positive ions depends on $\alpha_0$, $\delta$, $\gamma_+$, $\gamma_-$, and $a$ (the positive ion current). Integrating this equation with the initial condition $u$=0 at $\eta$=0, we obtain $u$ as a function of $\eta$. The integration needs a fixed value $a$. Figure 1 shows the evolution of $u$ with $\eta$ for $a$=90, $\gamma_+$=30, $\gamma_-$=10, $\delta$=0.5. With smaller values of $a$ (corresponding to the cases in this work), the slope of the curves becomes smaller. The evolution of $u$ with $\eta$ has sensitive dependence on $\alpha_0$. However, the values of $\delta$, $\gamma_+$, and $\gamma_-$ have insignificant influence on the evolution of $u$ with $\eta$. With Eq. (15) we calculate $u$ at arbitrary $\xi$. These provide the initial conditions to the model Eqs. (7)–(10).

In order to obtain the theoretical $I-V$ characteristic curve of the probe, Eqs. (8), (12), and (14) have been used. However, in that approach, the spatial distribution of the positive ion density cannot be accurately modeled because a simple flux conservation is assumed [in Eq. (12) with a given value of $a$]. On the other hand, in the model equations of this work, the positive ion current is an outcome result of the calculation rather than a control parameter.

For given values of the control parameters, the set of Eqs. (7)–(10) can be integrated from $\xi=\infty$ to any arbitrary small $\xi$. From the curve of the electric potential, the probe radius, $\xi=\xi_p$, determines the normalized potential $\eta_p$ for a given value of $a$. Note that both $a$ and $\xi_p$ depend on the unknown density $n_0$, which is to be determined from the measured current, but the value of $I=a\xi_p$ is independent of $n_0$. By computing a family of curves for different $a$, one can obtain $I-\eta_p$ curve for a probe of radius $\xi_p$. From selected values of $I$ and $\eta_p$ on the measured probe characteristics we have to estimate $\xi_p$. The electron temperature is supposed to be determined from measuring the slope of the experimental $I-V$ curve of the probe. Then it is possible to determine the plasma density, $\alpha_0$, and $\gamma_\pm$.

In this work, sheath refers to the region surrounding the probe where positive space charge exists, that is, this region includes the ion sheath where the electron density is negligible and the transition region where the electron density cannot be neglected but quasineutrality can never be applied.[23] The sheath edge marks the point where quasineutrality breaks.

## III. RESULTS AND DISCUSSION

The main focus of this paper is to investigate the effects of collision and finite thermal motion of the positive ions on the spatial distributions of the potential and the positive ion density. For that purpose, Eqs. (7)–(10) are solved numerically by using the fourth-order Runge–Kutta method with the initial condition which is obtained by solving the quasineutral Eqs. (15) and (16).

It is very difficult to integrate Eqs. (7)–(10) from $\xi=\infty$. Instead, a choice of $\xi$=100 as the plasma region is made based on the fact that 100 $\lambda_D$ is much larger than the sheath width. We have tried several values for the upper limit of integration and found that the numerical solutions are quite stable and reasonable for the choice of 100 $\lambda_D$. With a choice of a shorter upper limit than this, the solutions exhibit oscillatory structure and give unrealistic values.

As an example of the electronegative plasma, we can consider an oxygen discharge with $p$=1 mTorr, $T_e$=2.6 eV, $n_e=5.6\times10^{11}$ cm$^{-3}$, and $\lambda_D$=0.0016 cm, and we have $c_s=2.5\times10^5$ cm/s, $\nu_{iz}=10^6$ 1/s, $\Lambda$=0.25 cm, and $q$=0.006. For plasmas with higher electron temperature than this, the $\Lambda$ has a larger value but $q$ remains unchanged. The spatial distributions of the normalized potential, the normalized density, and the normalized velocity and flux of positive ions entering the probe are calculated for various values of $q$, $\alpha_0$, $\delta$, $\gamma_+$, $\gamma_-$. These values are selected so as to be outside the region in which potential oscillations are seen.[7,8,10] The effects of the $\delta$, $\gamma_+$, and $q$ on the radial profiles of electric potential, velocity and density of positive ions toward the probe are investigated.

Figures 2(a) and 2(b) show the normalized potential and the normalized velocity of positive ions along the distance from the plasma ($\xi$=100) to the probe ($\xi$ approaches zero) for various values of $\gamma_+$ with $q$=0.006. Although $\xi$ is cut off at 60 in the figures, the calculation is proceeded up to zero. In the figures, the $\xi$ coordinate is truncated to the point $\xi$=60, since the variations of the variables show the same pattern below the point. As $\gamma_+$ increases (as the positive ion temperature becomes lower), the sheath width increases. In other words, if the positive ions have larger thermal motion, the electric potential and the velocity of positive ion increase more slowly (going from the plasma to the probe), the sheath is contracted, and the ion current collected by the probe

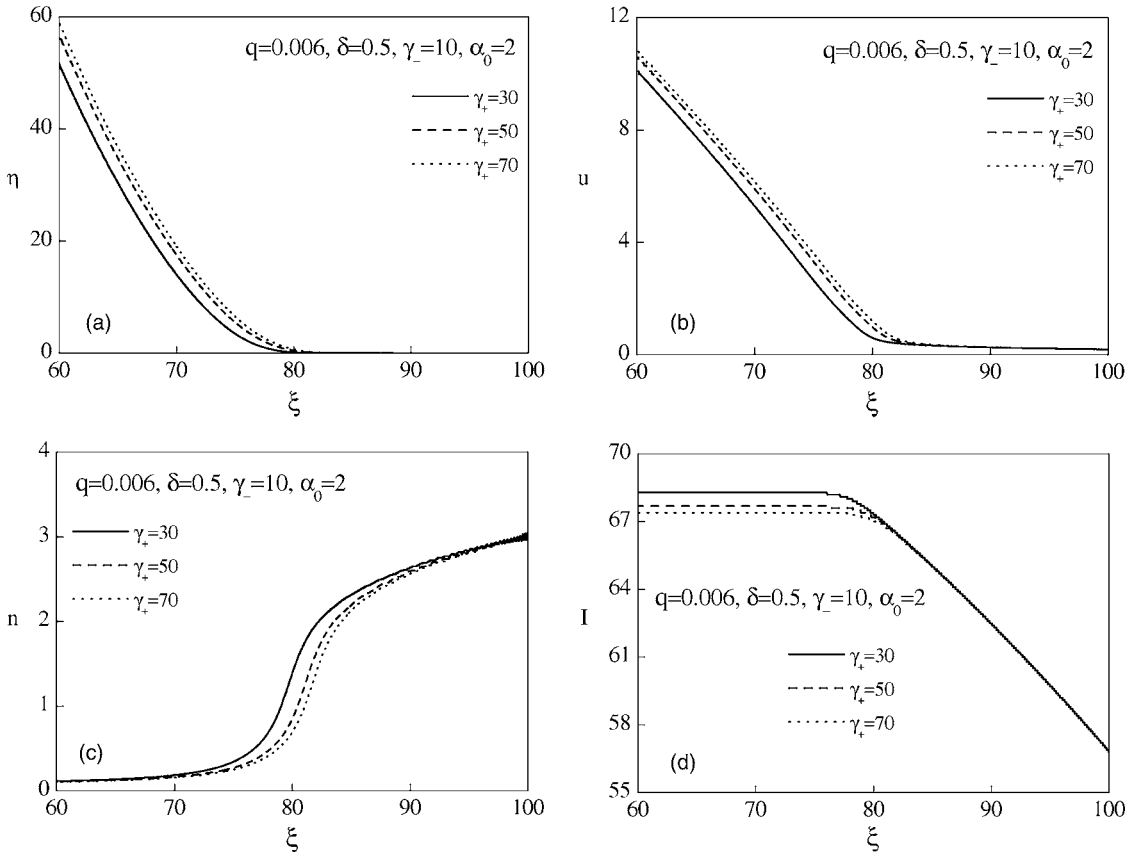


FIG. 2. (a) Normalized potential, (b) normalized velocity, (c) normalized density, and (d) normalized current of positive ions along the normalized distance for various positive ion temperatures ($\gamma_+=30$, 50, and 70). Here $q=0.006$, $\alpha_0=2$, $\gamma_-=10$, $\delta=0.5$.

increases.[18] Here, the sheath edge can also be defined as either the point at which the electric potential vanishes or the point at which the positive ions reach the speed of sound in the medium (the supersonic ion criterion).[9]

Figure 2(c) shows the normalized density of positive ions along the distance for various parameter values of $\gamma_+$. It is observed that the density profile of positive ion decreases rapidly toward the probe as $\gamma_+$ increases. The profiles have a largest slope at the sheath edge.

Figure 2(d) shows the calculated $\xi\tilde{n}u[=I(\xi)]$ as defined in Eq. (12), representing the normalized positive ion current. The results indicate that as $\gamma_+$ increases, the positive ion current collected by the probe decreases. It is observed that the calculated $I(\xi)$ values remain constant throughout the sheath region and therefore $a$ in Eq. (12) can be considered a constant. This allows the ABR theory to be valid for most of the parameter region of interest. The location of the sheath edge can be found to be consistent in the graphs of plasma variables [(a)–(d) of the figure].

Figures 3(a) and 3(b) show the normalized potential and normalized velocity of positive ions along the distance for various $\delta$ with $q=0.006$. The $\delta$ indicates the ratio of the rate coefficient for momentum transfer collision to that for the ionization. This value defines the collisionality of the plasma and is small at low pressure, being of the order of 1 and of the order of 1000 at higher pressure.[24,25] As $\delta$ increases, the sheath edge approaches the plasma region; thus, the sheath width increases. The increase in $\delta$ (collision term) causes the electric potential to increase more rapidly and the velocity to increase slightly faster (going from the plasma to the probe).

Figure 3(c) shows the normalized density of positive ions along the distance for various $\delta$. It is observed that the density profile of positive ion decreases drastically toward the probe and the sheath edge expands as $\delta$ increases. Figure 3(d) shows the calculated $I(\xi)$ for several $\delta$. The results show that as $\delta$ increases, the positive ion current to the probe decreases.

The normalized electric potential and normalized velocity of positive ions along the distance corresponding to the three different $\alpha_0$ values (=1,2,5) are shown in Figs. 4(a) and 4(b). For plasmas with very small $\alpha_0$, the interpretation of $I-V$ data may well follow that of the electropositive case. For plasmas with larger $\alpha_0$ than 10, the plasma parameters can easily be obtained by applying the double probe to the electronegative plasmas. As $\alpha_0$ increases, the potential increases to higher values and $\xi$ extends to larger values. This indicates that the sheath width expands as $\alpha_0$ increases. This result is in contradiction to the results of Crespo *et al.*[9] but is in agreement with the results of Amemiya *et al.*[6] Previous study of the author is also supportive of the latter work.[13] Figure 4(c) shows the density profiles of positive ions for various $\alpha_0$. It is observed that the density profile of positive ion decreases drastically toward the probe, and the sheath edge expands as $\alpha_0$ increases. Figure 4(d) shows the calculated $I(\xi)$ for several $\alpha_0$. The results show that as $\alpha_0$ increases, the positive ion current to the probe increases since

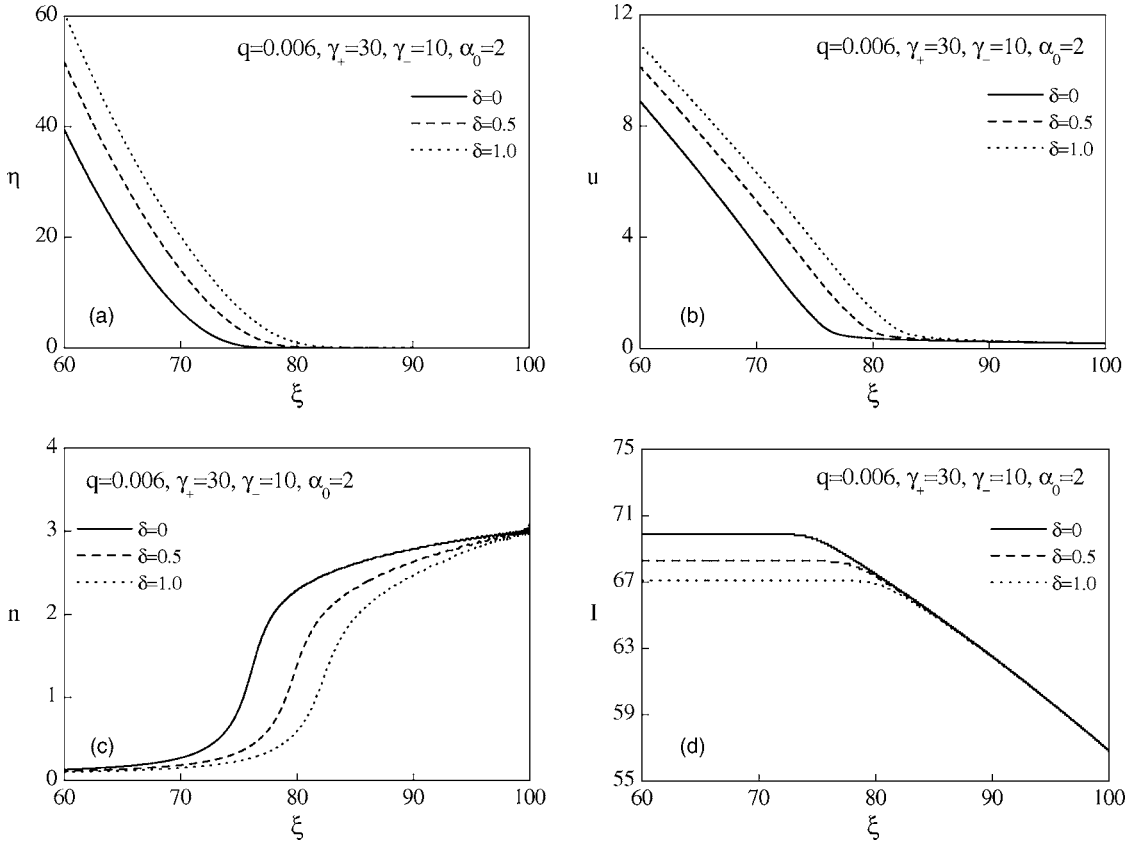


FIG. 3. (a) Normalized potential, (b) normalized velocity, (c) normalized density, and (d) normalized current of positive ions along the normalized distance for various collision parameters ($\delta$=0, 0.5, and 1.0). Here $q$=0.006, $\alpha_0$=2, $\gamma_-$=10, $\gamma_+$=30.

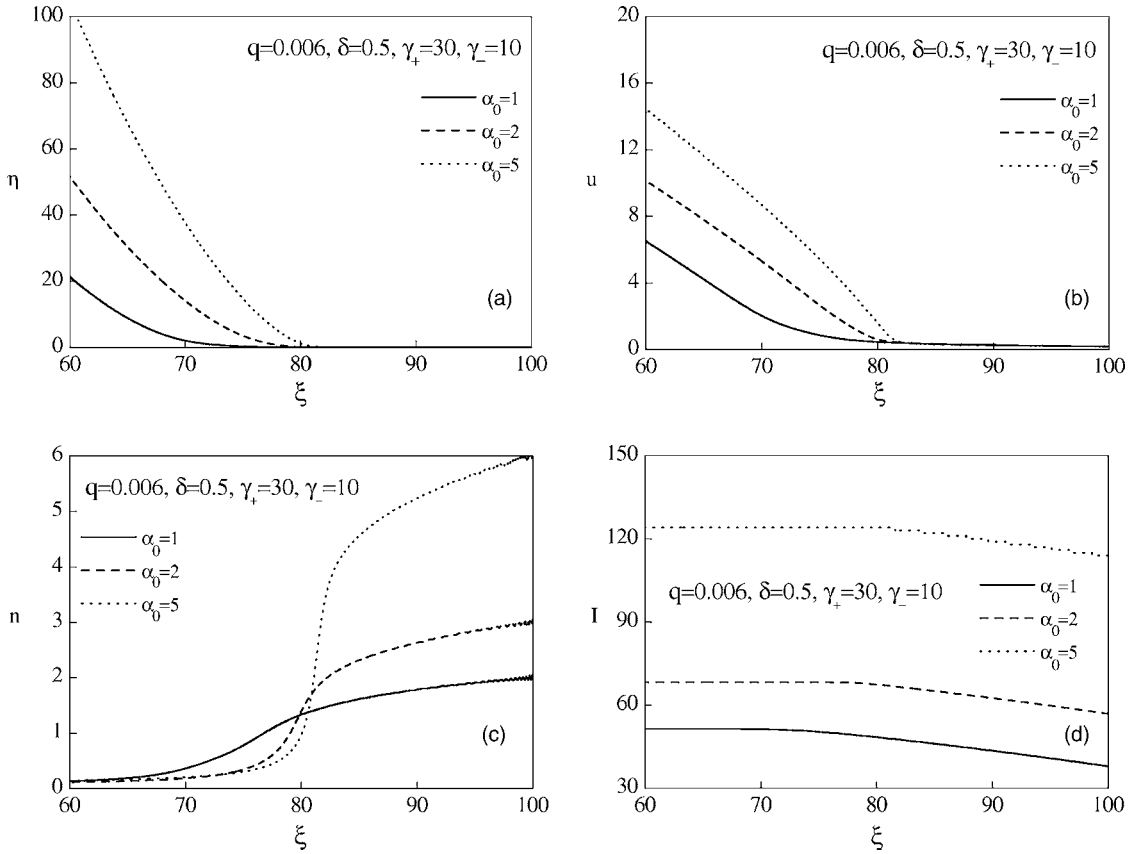


FIG. 4. (a) Normalized potential, (b) normalized velocity, (c) normalized density, and (d) normalized current of positive ions along the normalized distance for various $\alpha_0$ values ($\alpha_0$=1, 2, and 5). Here $q$=0.006, $\gamma_-$=10, $\gamma_+$=30, $\delta$=0.5.

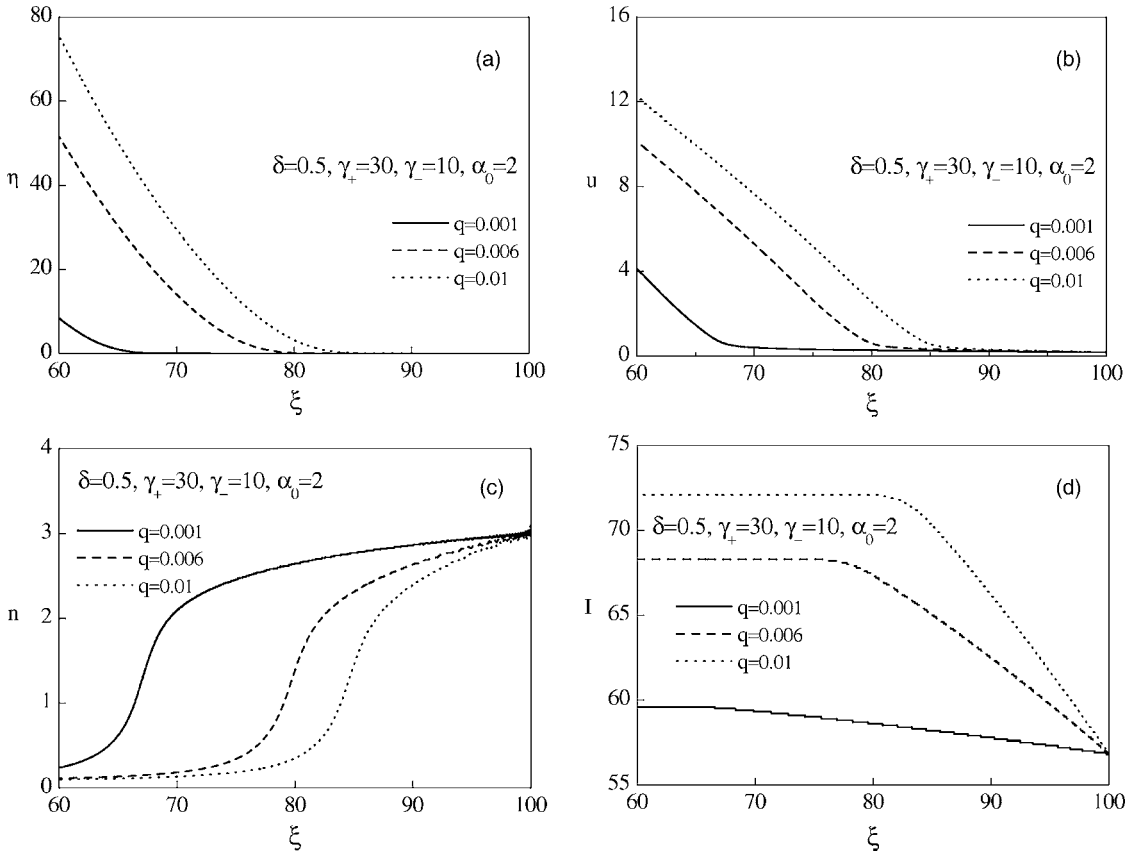


FIG. 5. (a) Normalized potential, (b) normalized velocity, (c) normalized density, and (d) normalized current of positive ions along the normalized distance for various $q$ values ($q$=0.001, 0.006, and 0.01). Here $\alpha_0$=2, $\gamma_-$=10, $\gamma_+$=30, $\delta$=0.5.

the initial value of the normalized density is $1+\alpha_0$. However, with the normalization by $1+\alpha_0$, the results indicate that a lower $\alpha_0$ case produces a larger positive ion current.

Figures 5(a) and 5(b) show the profiles of the electric potential and normalized velocity of positive ions for three different $q$. As $q$ increases, the electric potential increases more rapidly (going from the plasma to the probe) and the sheath width is found to increase. Also, as $q$ increases the velocity of the positive ion gets larger. Figure 5(c) shows the normalized density of positive ions along the distance for various $q$. It is observed that the density profile of positive ion decreases rapidly toward the probe as $q$ increases. From Fig. 5(d), it is seen that the positive ion current collected by the probe increases with increasing $q$, since larger $q$ results in more positive ion production by ionization. It can be stated that as $q$ increases the sheath width is found to increase, but the positive ion current collected by the probe increases. The applicability of this model is limited to the case of thin sheaths where the Debye length is much lower than the probe radius, because this model neglects the orbital motion of the ions. As the value of $q$ increases, the electron temperature and thus the sheath width increase; therefore, this model is not valid in large $q$ regions.

Although this model can give quite a clear picture of sheath region and the location of sheath edge for various set of plasma parameters and it allows us to estimate the positive ion current easily, it has some drawback in predicting the probe $I-V$ characteristics accurately. For one reason, the model in the present work may not precisely describe the positive ion motion in the sheath region because the assumptions made in formulating the model equations and the condition of constant parameters might not be valid in the sheath region. Complexities may occur when there is more than one species of positive or negative charge in the plasma. In addition, a kinetic analysis has to be performed to take into accounts of the effects of ion orbital motion, ion trapping in the sheath, and the finite length of the cylindrical probe, because in the collisional limit, the correct expression for the ion saturation current on a cylindrical probe should contain a logarithmic term accounting for finite length of the probe.

## IV. CONCLUSION

The spatial distributions of electric potential and velocity and density of positive ions are calculated in the surroundings of a negatively biased cylindrical probe immersed in electronegative plasmas. The model equations are solved on the scale of the electron Debye length. The control parameters are the ratio of the negative ion density to the electron density, the ratios of the electron temperature to the positive and negative ion temperatures, and the ratio of the rate coefficient for the momentum transfer collision to that for the ionization. The solutions provide the variation of plasma variables along the distance from the plasma bulk region to the probe surface. The effects of collision and finite thermal motion of positive ions are investigated. If the positive ions have larger thermal motion, the electric potential increases more slowly, the sheath is contracted, and the positive ion

current collected by the probe increases. The increase of collision causes the electric potential to increase more rapidly and the sheath to be enlarged, resulting in a decrease in the positive ion current. As the value of the non-neutrality parameter $q$ increases, the sheath width is found to increase but the positive ion current collected by the probe increases. The merit of this model lies in giving a clear picture of sheath region and easy calculation of the positive ion current. The location of sheath edge can be seen consistently in various plasma variables.

## ACKNOWLEDGMENTS

This work is supported by Hanbit User Program of Korea National Fusion Research Institute in the program year of 2005–2007.

[1]T. H. Chung, H. J. Yoon, and D. C. Seo, J. Appl. Phys. **86**, 3536 (1999).
[2]T. H. Chung, D. C. Seo, G. H. Kim, and J. S. Kim, IEEE Trans. Plasma Sci. **29**, 970 (2001).
[3]D. C. Seo, T. H. Chung, H. J. Yoon, and G. H. Kim, J. Appl. Phys. **89**, 4218 (2001).
[4]F. Taccogna, S. Longo, and M. Capitelli, Contrib. Plasma Phys. **44**, 594 (2004).
[5]R. Morales Crespo, J. I. Fernandez Palop, M. A. Hernandez, and J. Ballesteros, J. Appl. Phys. **95**, 2982 (2004).
[6]H. Amemiya, B. M. Annaratone, and J. E. Allen, Plasma Sources Sci. Technol. **8**, 179 (1999).
[7]R. N. Franklin, Plasma Sources Sci. Technol. **9**, 191 (2000).
[8]T. E. Sheridan, P. Chabert, and R. W. Boswell, Plasma Sources Sci. Technol. **8**, 457 (1999).
[9]R. Morales Crespo, J. I. Fernandez Palop, M. A. Hernandez, S. Borrego del Pino, and J. Ballesteros, J. Appl. Phys. **96**, 4777 (2004).
[10]A. Kono, J. Phys. D **32**, 1357 (1999).
[11]A. Kono, J. Phys. D **34**, 1083 (2001).
[12]A. Kono, J. Phys. D **36**, 465 (2003).
[13]T. H. Chung, Phys. Plasmas **13**, 024501 (2006).
[14]J. I. Fernandez Palop, J. Ballesteros, R. Morales Crespo, and M. A. Hernandez, Appl. Phys. Lett. **88**, 261502 (2006).
[15]J. I. Fernandez Palop, J. Ballesteros, M. A. Hernandez, R. Morales Crespo, and S. Borrego del Pino, J. Phys. D **37**, 863 (2004).
[16]J. I. Fernandez Palop, J. Ballesteros, M. A. Hernandez, R. Morales Crespo, and S. Borrego del Pino, J. Phys. D **38**, 868 (2005).
[17]R. Morales Crespo, J. I. Fernandez Palop, M. A. Hernandez, S. Borrego del Pino, J. M. Diaz-Cabrera, and J. Ballesteros, J. Appl. Phys. **99**, 053303 (2006).
[18]J. I. Fernandez Palop, J. Ballesteros, M. A. Hernandez, R. Morales Crespo, and S. Borrego del Pino, J. Appl. Phys. **95**, 4585 (2004).
[19]K. U. Riemann, IEEE Trans. Plasma Sci. **23**, 709 (1995).
[20]J. E. Allen, R. L. F. Boyd, and P. Reynolds, Proc. Phys. Soc. London, Sect. B **70**, 297 (1957).
[21]F. F. Chen, J. Nucl. Energy **7**, (Part C), 47 (1965).
[22]J. I. Fernandez Palop, J. Ballesteros, V. Colomer, and M. A. Hernandez, J. Phys. D **29**, 2832 (1996).
[23]F. Iza and J. K. Lee, J. Vac. Sci. Technol. A **24**, 1366 (2006).
[24]R. N. Franklin and J. Snell, J. Phys. D **33**, 1990 (2000).
[25]R. N. Franklin, J. Phys. D **36**, 2821 (2003).